Homodinuclear lanthanoid(III) dithiocarbamato complexes bridged by 2,2'-bipyrimidine: syntheses, structures and spectroscopic properties

Abdallah Yakubu,[a] Takayoshi Suzuki,[a,b,*] Masakazu Kita[c]

[a] Graduate School of Natural Science and Technology, Okayama University, 3-1-1 Tsushima-naka, Kita-ku, Okayama 700-8530, Japan

[b] Research Institute for Interdisciplinary Science, Okayama University, 3-1-1 Tsushima-naka, Kita-ku, Okayama 700-8530, Japan

[c] Faculty of Education, Okayama University, 3-1-1 Tsushima-naka, Kita-ku, Okayama 700-8530, Japan

Abstract

Four new homodinuclear lanthanoid(III) dithiocarbamato (*RR*′dtc^{-}) complexes bridged by 2,2'-bipyrimidine (bpm) of the form [{Ln(*RR*′dtc)$_3$}$_2$(μ-bpm)] {Ln = Nd or Eu; *RR*′ = dimethyl- (Me_2) or pyrrolidine- (pyr)} were prepared and their crystal structures and spectroscopic properties were characterized. Crystallographic studies revealed that all of the complexes possess a similar structural motif with an 8:8-coordination geometry, in which bpm bridges two Ln^{III} centers in the $\kappa^2N^{1,1'}$:$\kappa^2N^{3,3'}$ mode and three *RR*′dtc^{-} ligands coordinate to each Ln^{III} center. The complexes exhibited weak but relatively sharp f–f transition bands in the absorption and magnetic circular dichroism (MCD) spectra recorded in the visible region. The MCD spectral studies demonstrated the magneto-optical behavior of the complexes. The spectral features of the dithiocarbamato complexes were distinctly different from those of the β-diketonato analogues, suggesting the coordination environment around the Ln^{III} center influences the electronic structure and spectroscopic symmetry of the complexes in solution.

Keywords: 2,2'-bipyrimidine, dithiocarbamate, homodinuclear, electronic structure, magnetic circular dichroism.

1. Introduction

The role of homo- and hetero-dinuclear lanthanoid complexes as building blocks for coordination polymers and supramolecular assemblies is a significant field of study in recent years. Dinuclear lanthanoid complexes with intriguing structural diversity, spectroscopic, magnetic and physicochemical properties have been studied for many reasons including catalysis, optical probes, magnetic materials, biological assays, display devices, and microelectronics [1,2]. Many dinuclear complexes and coordination polymers with a variety of bridging ligands have been reported [3], and 2,2'-bipyrimidine (bpm) is one of the heterocyclic bridging ligands, which have been shown to afford diverse structural architectures with different dimensionalities [3,4]. The coordination chemistry of polyazine bridging ligands and transition metals is a well-established field of study [2], but it is only recently that the coordination ability of bpm to form complexes with lanthanoids has been explored [4]. In addition to studies on the structures and photophysical properties of heterometallic d-f systems [5,6], several examples of homodinuclear lanthanoid complexes bearing β-diketonato co-ligands appeared in the literature. D'Cunha et al. reported the synthesis of homodinuclear lanthanoid complexes bridged by bpm and capped with terminal β-diketonato ligands [7]. Yu et al. have reported the molecular structures and magnetic properties of bpm bridged homodinuclear lanthanoid complexes of 2,2',6,6'-tetramethyl-3,5-heptanedionate [8]. Sun et al. have reported the single-molecule magnetic behavior of bpm bridged Dy^{III}_2 β-diketonato dimers [9]. Absorption and photoluminescence properties of bpm-bridged homodinuclear lanthanoid(III) 2,4-pantanedionato complexes have also been reported [10]. On the other hand, the analogous lanthanoid chemistry with dithiocarbamato co-ligands and polyazine bridging ligands has not yet been studied.

Lanthanoid dithiocarbamato complexes have been studied sporadically since the 1960s. However, interests in these complexes have recently resurfaced for practical applications in catalysis, nanotechnology, and microelectronics [11,12]. For examples, syntheses, crystallographic and spectroscopic characterizations of mononuclear lanthanoid complexes of various dialkyl-substituted dithiocarbamates with 1,10-phenanthroline (phen) and 2,2'-bipyridine (bpy) have been reported [13-17]. In a previous study [17], we have investigated the

crystal structures and spectroscopic properties of the Nd^{III} and Eu^{III} complexes containing chiral or achiral dithiocarbamates. In particular, their natural circular dichroism (CD) and magnetic circular dichroism (MCD) spectra were discussed in relation to the coordination environment and electronic structure around the lanthanoid center, because Nd^{III} and Eu^{III} often give representative examples showing CD- and MCD-active f–f transitions bands. In this study, we will describe four new homodinuclear lanthanoid dithiocarbamato complexes using 2,2'-bipyrimidine (bpm) as a bridging unit, and compare their structures and spectroscopic properties with those of the mononuclear phen or bpy complexes and with those of the corresponding dinuclear β-diketonato complexes.

2. Experimental section

2.1 Synthesis of Dithiocarbamato Complexes

The complexes were prepared by a similar procedure (Scheme 1) to that for mononuclear 2,2'-bipyridine (bpy) and 1,10-phenanthroline (phen) complexes [17]. To a mixture of 2,2'-bipyrimidine, bpm (1.00 mmol) and sodium dimethyldithiocarbamate, $Na(Me_2dtc)$ or ammonium pyrrolidine dithiocarbamate, $NH_4(pyrdtc)$ (3.00 mmol) in MeOH (20 mL) was added a methanol solution (10 mL) of $LnCl_3 \cdot 6H_2O$ (Ln = Nd or Eu) (1.00 mmol). The mixture was stirred for 4 h at room temperature and the resulting precipitate was collected by filtration, washed with MeOH and dried in air. The crude product was purified by recrystallization. The method of recrystallization, the results of elemental analysis and the FT-IR spectral data of respective complexes are given below.

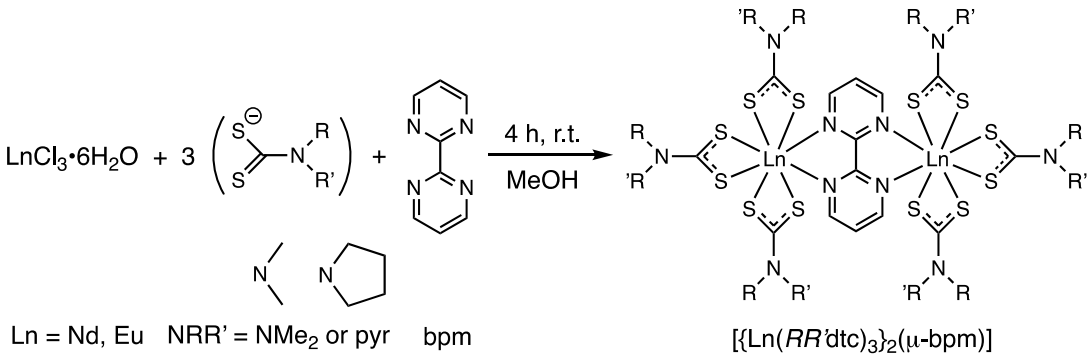

Scheme 1 Synthesis of $[\{Ln(RR'dtc)_3\}_2(\mu\text{-bpm})]$ complexes.

2.1.1 [{Nd(Me$_2$dtc)$_3$}$_2$(μ-bpm)] (**1a**)

Green crystals were grown from a CH_2Cl_2 solution layered with Et_2O in 37% yield, while single-crystals suitable for X-ray diffraction analysis were obtained from $CHCl_3$/Et_2O. Anal. Found: C, 25.04; H, 3.67; N, 10.57; S, 29.06%. Calcd. for $C_{26}H_{42}N_{10}Nd_2S_{12}\cdot 2CH_2Cl_2$: C, 25.14; H, 3.47; N, 10.47; S, 28.76%. IR (KBr disc) cm^{-1}: *ν*(C–N) 1374; *ν*(C–S) 983.

2.1.2 [{Nd(pyrdtc)$_3$}$_2$(μ-bpm)] (**1b**)

Greenish-yellow crystals were obtained from a mixture of $CHCl_3$ and EtOH in 46% yield. Anal. Found: C, 33.34; H, 3.99; N, 9.97; S, 27.18%. Calcd. for $C_{38}H_{54}N_{10}Nd_2S_{12}\cdot 0.5CHCl_3$: C, 33.41; H, 3.97; N, 10.12; S, 27.81%. IR (KBr disc) cm^{-1}: *ν*(C–N) 1436; *ν*(C–S) 948.

2.1.3 [{Eu(Me$_2$dtc)$_3$}$_2$(μ-bpm)] (**2a**)

Orange crystals were obtained from a mixture of CH_2Cl_2 and Et_2O in 38% yield, while single-crystals suitable for X-ray diffraction analysis were obtained from a mixture of $CHCl_3$ and Et_2O. Anal. Found: C, 24.39; H, 3.29; N, 10.56; S, 28.10%. Calcd. for $C_{26}H_{42}N_{10}Eu_2S_{12}\cdot 2CH_2Cl_2$: C, 24.85; H, 3.43; N, 10.35; S, 28.43%. IR (KBr disc) cm^{-1}: *ν*(C–N) 1399; *ν*(C–S) 984.

2.1.4 [Eu$_2$(pyrdtc)$_6$(μ-bpm)] (**2b**)

Orange crystals were obtained from a mixture of CH_2Cl_2 and Et_2O mixture in 48% yield, while single-crystals suitable for X-ray diffraction analysis were obtained from a CH_2Cl_2 solution by adding a 1:1 mixture of EtOH/Et_2O. Anal. Found: C, 34.28; H, 4.17; N, 10.35; S, 27.95%. Calcd. for $C_{38}H_{54}N_{10}Eu_2S_{12}$: C, 34.07; H, 4.06; N, 10.46; S, 28.72%. IR (KBr disc) cm^{-1}: *ν*(C–N) 1436; *ν*(C–S) 949.

2.2 Synthesis of Acetylacetonato Complexes

The complexes, [{Ln(acac)$_3$}$_2$(μ-bpm)] (Ln = Nd (**1c**) and Eu (**2c**)) were prepared, following the procedure described by Ilmi *et al*. with some modification [10]. To a mixture of 2,2'-bipyrimidine, bpm (0.50 mmol) and lithium acetylacetonate, Li(acac) (3.00 mmol) in absolute EtOH (20 mL) was added an absolute EtOH solution (10 mL) of $LnCl_3\cdot 6H_2O$ (1.00 mmol) (Ln = Nd or Eu). The mixture was stirred on a hot plate at an elevated temperature below the boiling point of the solvent for 4 h and the resulting solution (concentrated to ca. 15 mL) was filtered.

The filtrate was kept at room temperature for slow evaporation of the solvent. Single-crystals suitable for X-ray diffraction study were obtained within 24 h. The crystals were collected by filtration and dried in air.

2.3 Structural Characterization

X-ray diffraction data of all complexes were collected on a Rigaku R-AXIS Rapid diffractometer using a graphite-monochromatized Mo-Kα (λ = 0.71075Å) radiation. Data were collected and processed using a program package, process-auto [18]. The structures were solved by the direct methods [19,20] and expanded using Fourier techniques. The non-hydrogen atoms were refined anisotropically. Hydrogen atoms were introduced at theoretical positions and treated with the riding models. All calculations were performed using a program package, CrystalStructure [21], except for the refinement, which was performed using SHELXL Version 2014/7 [22].

2.4 Physical Measurements

C, H, N and S analysis of the complexes were carried out on a Perkin Elmer Series II CHNS/O Analyzer 2400 at Advanced Science Research Center, Okayama University. The FT-IR spectra were recorded on a JASCO FT-001 FT-IR spectrophotometer in KBr disc in the 4000–400 cm^{-1} range. The UV-visible absorption spectra of the complexes in a CH_2Cl_2 solution were obtained on a JASCO V-550 UV/VIS spectrophotometer at room temperature. Room temperature magnetic circular dichroism (MCD) spectra were measured on a JASCO J-1500 CD spectropolarimeter equipped with a home-made 0.5 T neodymium magnet [23].

3. Results and Discussion

3.1 Synthesis of 2,2'-bipyrimidine-bridged Ln^{III}_2 complexes

The 2,2'-bipyrimidine-bridged dinuclear lanthanoid(III) complexes with dithiocarbamato co-ligands were prepared by a one-pot reaction from $LnCl_3 \cdot 6H_2O$ (Ln = Nd^{III} (**1**) and Eu^{III} (**2**)), 2,2'-bipyrimidine (bpm) and sodium *N*,*N*-dimethyldithiocarbamate (Me_2dtc^-) or ammonium pyrrolidine dithiocarbamate ($pyrdtc^-$) in a 1:1:3 molar ratio in methanol at room temperature. These dithiocarbamato complexes were isolated in 37–48% yields. The acetylacetonato

analogues were prepared similarly by a reaction of $LnCl_3 \cdot 6H_2O$, bpm and lithium acetylacetonate ($acac^-$) in a 2:1:6 molar ratio in absolute ethanol at an elevated temperature, and isolated in 23–24% yields. All of the complexes prepared were characterized by elemental analyses, single-crystal X-ray diffraction analysis, FT-IR, absorption and magnetic circular dichroism (MCD) spectroscopy.

3.2 Crystal Structures

Single-crystal X-ray diffraction analysis revealed that all complexes investigated in this study, **1a**–**1c** and **2a**–**2c**, have a centrosymmetric homodinuclear structure. Complexes of $[\{Nd(Me_2dtc)_3\}_2(\mu\text{-bpm})]\cdot 2CHCl_3$ (**1a**$\cdot 2CHCl_3$) and $[\{Eu(Me_2dtc)_3\}_2(\mu\text{-bpm})]\cdot 2CHCl_3$ (**2a**$\cdot 2CHCl_3$) are isomorphous and crystallized in the monoclinic space group $P2_1/n$ with Z = 2, while $[\{Nd(pyrdtc)_3\}_2(\mu\text{-bpm})]\cdot 2CHCl_3$ (**1b**$\cdot 2CHCl_3$) crystallized in the monoclinic space group $C2/c$ with Z = 4. The corresponding Eu^{III}–pyrdtc complex, **2b**, afforded two kinds of pseudo-polymorphic crystals; the one is of the formula $[\{Eu(pyrdtc)_3\}_2(\mu\text{-bpm})]\cdot 4CH_2Cl_2$ (**2b**$\cdot 4CH_2Cl_2$) crystallized in the monoclinic space group $C2/c$ with Z = 4, and the other of $[\{Eu(pyrdtc)_3\}_2(\mu\text{-bpm})]\cdot CH_2Cl_2$ (**2b**$\cdot CH_2Cl_2$) in the triclinic space group $P\bar{1}$ with Z = 2. The acetylacetonato analogues, $[\{Nd(acac)_3\}_2(\mu\text{-bpm})]$ (**1c**) and $[\{Eu(acac)_3\}_2(\mu\text{-bpm})]$ (**2c**), are also isomorphous and crystallized in the triclinic space group $P\bar{1}$ with Z = 1, although the crystallographic data of **2c** has been reported previously [24]. The crystallographic data of the complexes **1a**–**1c**, **2a** and **2b** (both crystals) are summarized in Table 1, while selected bond parameters of them are listed in Table S1.

The molecular structures of **1a** and **2a** have a similar core structure (Figure 1), in which each Ln^{III} center is 8-coordinated by three bidentate *S*,*S*-donating Me_2dtc^- ligands with a chelating and bridging bpm ligand in a $\kappa^2N^{1,1'}:\kappa^2N^{3,3'}$ bonding mode. The coordination geometry around each Ln^{III} center is similar to those of previously reported 1,10-phenathroline and 2,2'-bipyridine coordinated mononuclear analogues [17]. The two pyrimidine rings of the bridging bpm ligand are almost planar (mean deviation of each atom from the plane is 0.010(5) Å in **1a**$\cdot 2CHCl_3$ and 0.008(7) Å in **2a**$\cdot 2CHCl_3$) [25]. The Ln^{III} atom is located slightly above the bpm ligand plane by 0.262(9) and 0.272(9) Å in **1a**$\cdot 2CHCl_3$ and **2a**$\cdot 2CHCl_3$, respectively.

The pseudo *trans*-positioned Me_2dtc ligand plane is slightly tilted from the bridging bpm plane with the dihedral angles of 14.09(5) and 15.22(5)° in **1a**·2$CHCl_3$ and **2a**·2$CHCl_3$, respectively. The other set of mutually pseudo *trans*-positioned Me_2dtc ligands, which are perpendicular to the bridging bpm plane, are co-planar to each other with the dihedral angles of 5.16(5) and 5.90(1)° in **1a**·2$CHCl_3$ and **2a**·2$CHCl_3$, respectively (Figure 1*b*). The intramolecular Ln···Ln distances across the bridging bpm ligand are 6.9744(5) Å in **1a**·2$CHCl_3$ and 6.8602(6) Å in **2a**·2$CHCl_3$.

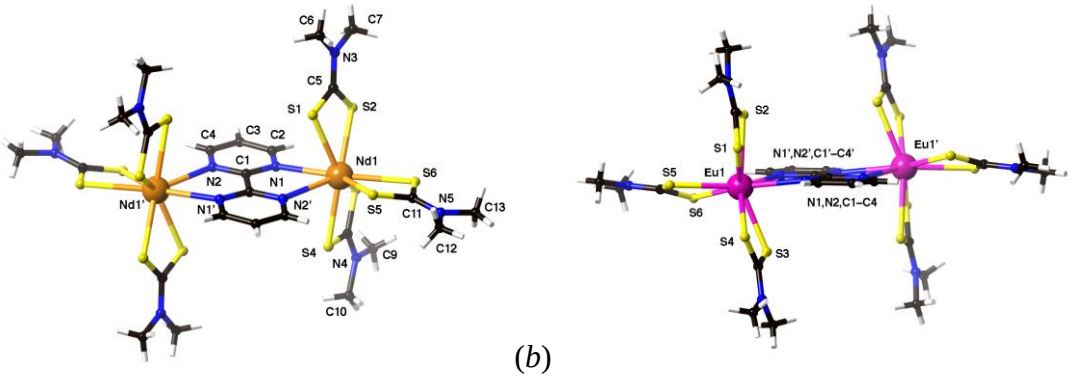

(*a*) (*b*)

Figure 1. (a) A perspective view of [{Nd(Me_2dtc)$_3$}$_2$(μ-bpm)] (**1a**) with atom-numbering scheme. (b) A view of [{Eu(Me_2dtc)$_3$}$_2$(μ-bpm)] (**2a**) from a direction parallel to the bridging bpm and the mutually *trans*-positioned Me_2dtc ligand planes.

In the case of pyrdtc complexes, three pseudo-polymorphs with different kinds and/or number of solvent molecules of crystallization were analyzed by the X-ray diffraction method: the Nd^{III} complex with two $CHCl_3$ molecules, **1b**·2$CHCl_3$, and the Eu^{III} complex with four or one CH_2Cl_2 molecule(s), **2b**·4CH_2Cl_2 and **2b**·CH_2Cl_2. The molecular structure of bpm-bridged dinuclear Nd^{III} complex in **1b**·2$CHCl_3$ is illustrated in Figure 2, and those of the corresponding Eu^{III} complexes in **2b**·4CH_2Cl_2 and **2b**·CH_2Cl_2 are in Figure 3. The overall structural characteristics of dinuclear [{Eu(pyrdtc)$_3$}$_2$(μ-bpm)] complex in **2b**·4CH_2Cl_2 (Figure 3*a*) is similar to those of the above-mentioned Me_2dtc complexes in **1a**·2$CHCl_3$ and **2a**·2$CHCl_3$ (Figure 1) and the corresponding mononuclear pyrdtc complexes with bpy or phen co-ligand [17]. In **2b**·4CH_2Cl_2 the Eu^{III} atom is located on the bridging-bpm ligand plane, the deviation being only 0.059(5) Å. The dihedral angle between the bridging-bpm and its pseudo *trans*-positioned pyrdtc ligand planes is 35.27(8)° in **2b**·4CH_2Cl_2, while the mutually *trans*-

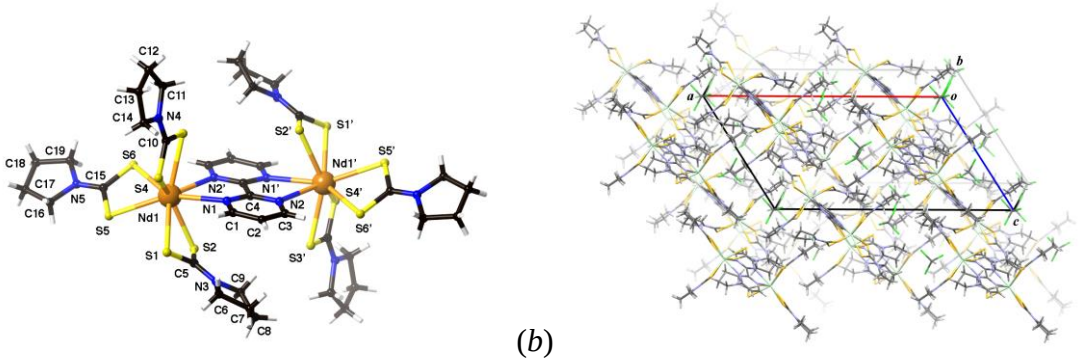

(*a*) (*b*)

Figure 2. (*a*) Molecular structures of [{Nd(pyrdtc)$_3$}$_2$(μ-bpm)] in **1b**·2CHCl$_3$ with atom-numbering scheme and (*b*) a packing diagram of **1b**·2CHCl$_3$.

positioned pyrdtc ligand planes are almost co-planar, the dihedral angle between them being 12.91(1)°. In contrast, the Nd^{III} complex in **1b**·2CHCl$_3$ gave a severe structural distortion for one of the coordinated pyrdtc ligands, as shown in Figure 2*a*. The dihedral angle between the mutually *trans*-positioned pyrdtc ligand planes is as large as 53.71(7)°. In addition, the Nd^{III} atom is deviated by 0.327(9) Å from the bridging-bpm plane. Other structural parameters as

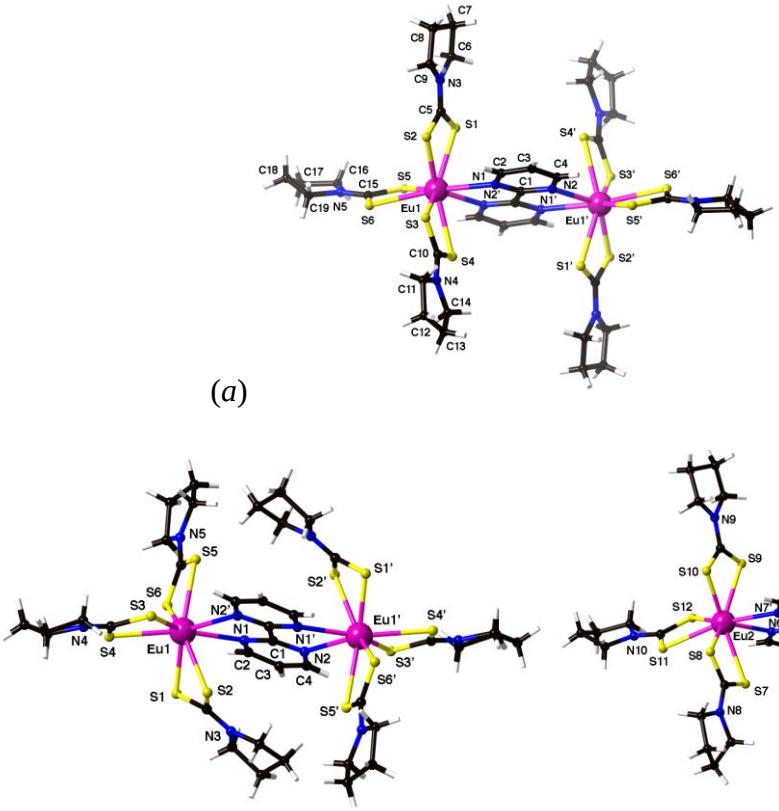

(*a*)

(*b*)

Figure 3. (*a*) A perspective view of [{Eu(pyrdtc)$_3$}$_2$(μ-bpm)] in **2b**·4CH$_2$Cl$_2$ and (*b*) those of two crystallographically independent complex molecules in **2b**·CH$_2$Cl$_2$.

well as the coordination geometry around Nd^{III} center is similar to those of the non-distorted Eu^{III} complex in **2b**·$4CH_2Cl_2$; the equatorial-positioned pyrdtc plane is twisted out of the bridging-bpm plane by 34.02(4)° in **1b**·$2CHCl_3$. The characteristic distortion is possibly due either to the intramolecular π–π stacking interaction between the bpm and pyrdtc ligands or to the packing effects from the solvent $CHCl_3$ molecule (Figure 2*b*). Interestingly, the crystal of **2b**·CH_2Cl_2 contains both structural types of dinuclear Eu^{III} complexes (Figure 3*b*), although the accuracy of the analysis was not perfect due to its poor crystallinity. In this triclinic crystal (space group $P\bar{1}$ with $Z = 2$) the asymmetric unit consists of two half-molecules of the bpm-bridged dinuclear Eu^{III} complexes and a CH_2Cl_2 molecule of crystallization, and one of the dinuclear complex having Eu1 showed a distorted structural feature similar to that of the above-mentioned Nd^{III} complex in **1b**·$2CHCl_3$, while the other having Eu2 gave a non-distorted structure as in **2b**·$4CH_2Cl_2$. The intramolecular $Ln^{III}\cdots Ln^{III}$ distances across the bridging bpm ligand is 6.9908(5) Å in **1b**·$2CHCl_3$, 6.8673(4) Å in **2b**·$4CH_2Cl_2$, and 6.832(1) and 6.848(1) Å in **2b**·CH_2Cl_2. The average Ln^{III}–S bond lengths in **1a**–**2b**, 2.831(4)–2.869(4) Å, are in good agreement with the corresponding values reported for the mononuclear analogues with phen or bpy co-ligand. On the other hand, the average Ln^{III}–N bond lengths in **1a**–**2b**, 2.620(6)–2.672(6) are longer than those in the mononuclear phen complexes [17]. This difference in the Ln^{III}–N(bpm) and Ln^{III}–N(phen) bond lengths may be related to the less pronounced basic character of bpm [1,4].

As a structural comparison, the crystal structure of the analogous acac complex **1c** is illustrated in Figure 4, while that of **2c** was reported previously [24]. Each Nd^{III} center has a similar coordination geometry to that of the Me_2dtc complex, **1a**, described above. A characteristic difference between **1a** and **1c** was found in the coordination geometry around the Nd^{III} center; in contrast to the structure shown in Figure 1*b*, the bridging bpm and the pseudo *trans*-positioned acac ligand planes of complex **1c** are almost co-planar as depicted in Figure 4*b*. The dihedral angle between these ligand planes is only 5.24(4)°. The intramolecular Nd···Nd distance across the bridging bpm ligand of 7.0702(5) Å in **1c** is slightly longer than the corresponding values in **1a** and **1b**. The Ln–N length of 2.704(3) Å in **1c** is in good agreement with those of **1a** and **1b**.

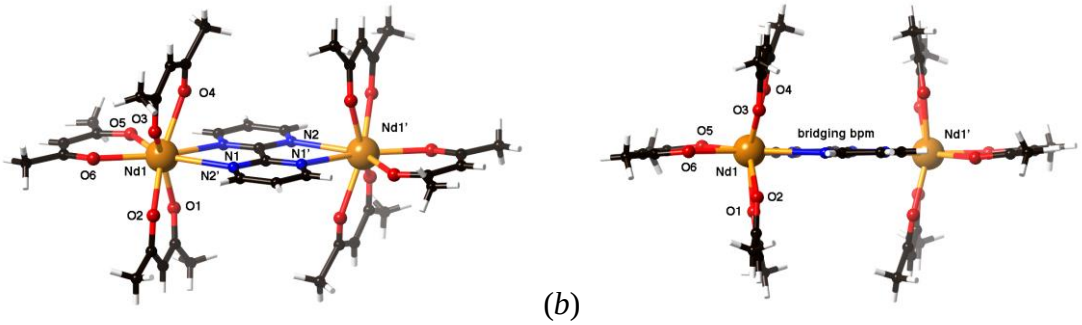

(*a*) (*b*)

Figure 4.(a) A perspective view of [{Nd(acac)$_3$}$_2$(μ-bpm)] (**1c**) and (b) a view of the same complex from a direction parallel to the bridging bpm and the mutually *trans*-positioned acac ligand planes.

Table 1. Crystallographic data of dinuclear Ln_2^{III} complexes.

Parameter	**1a**·2CHCl$_3$	**1b**·2CHCl$_3$	**1c**
Molecular formula	$C_{28}H_{44}Cl_6N_{10}Nd_2S_{12}$	$C_{40}H_{56}N_{10}Cl_6Nd_2S_{12}$	$C_{38}H_{48}N_4Nd_2O_{12}$
Molecular weight	1406.64	1562.87	1041.30
Temperature (K)	188	188	188
Crystal system	Monoclinic	Monoclinic	Triclinic
Space group, Z	$P2_1/n$, 2	$C2/c$, 4	$P\bar{1}$, 1
a (Å)	16.0903(8)	27.2998(11)	9.3304(3)
b (Å)	11.1735(6)	18.0517(7)	10.1142(9)
c (Å)	16.6342(6)	15.3180(8)	12.4276(4)
α (°)	90	90	108.662(5)
β (°)	116.4757(15)	121.8007(14)	95.9487(17)
γ (°)	90	90	95.150(5)
V (Å^3)	2677.0(2)	6415.7(5)	1095.69(11)
D_{calcd} (g cm^{-3})	1.745	1.618	1.578
μ(Mo Kα) (cm^{-1})	27.177	22.770	24.022
F(000)	1392	3120	520
R_{int}	0.0715	0.0487	0.0440
$R1$ [$I > 2\sigma(I)$]	0.0458	0.0434	0.0256
$wR2$ [all data]	0.1275	0.1415	0.0894
GOF on F^2	1.066	1.058	1.237

Table 1. (Continued)

Parameter	**2a**·2$CHCl_3$	**2b**·4CH_2Cl_2	**2b**·CH_2Cl_2
Molecular formula	$C_{28}H_{44}Cl_6N_{10}Eu_2S_{12}$	$C_{42}H_{60}N_{10}Cl_8Eu_2S_{12}$	$C_{39}H_{56}N_{10}Cl_2Eu_2S_{12}$
Molecular weight	1422.08	1677.27	1424.47
Temperature (K)	188	188	188
Crystal system	Monoclinic	Monoclinic	Triclinic
Space group, Z	$P2_1/n$, 2	$C2/c$, 4	$P\bar{1}$, 2
a (Å)	16.0722(14)	24.4037(14)	10.7040(19)
b (Å)	11.0919(10)	17.9989(10)	15.200(3)
c (Å)	16.6771(14)	15.0300(9)	17.936(3)
α (°)	90	90	80.020(5)
β (°)	116.559(3)	94.5797(19)	73.696(5)
γ (°)	90	90	75.939(5)
V (Å^3)	2659.3(4)	6580.7(7)	2699.5(9)
D_{calcd} (g cm^{-3})	1.776	1.693	1.752
μ(Mo Kα) (cm^{-1})	31.378	26.287	29.06
F(000)	1404	3344	1424
R_{int}	0.1034	0.0463	0.1136
*R*1 [$I > 2\sigma(I)$]	0.0516	0.0291	0.0754
*wR*2 [all data]	0.1023	0.0714	0.2370
GOF on F^2	1.055	1.048	1.161

3.3 Spectroscopic studies

3.3.1 FT-IR Spectral Study

The infrared spectra of the complexes in the regions of 1450–1550 and 950–1050 cm^{-1} are of interest, because the *ν*(C–N) and *ν*(C–S) stretching bands are appeared in these regions [26,27]. The [{Nd(Me_2dtc)$_3$}$_2$(μ-bpm)] (**1a**) and [{Eu(Me_2dtc)$_3$}$_2$(μ-bpm)] (**2a**) complexes (Figure S1) exhibited the *ν*(C–N) band between 1374–1418 cm^{-1}, while [{Nd(pyrdtc)$_3$}$_2$(μ-bpm)] (**1b**) and [[{Eu(pyrdtc)$_3$}$_2$(μ-bpm)] (**2b**) complexes (Figure S2) showed the band around 1436 cm^{-1}. The *ν*(C–S) bands of the complexes above were observed in the range of 948–984 cm^{-1}. These band positions of the dinuclear complexes are consistent with those reported for the related mononuclear analogues [17].

3.3.2 Absorption and magnetic circular dichroism (MCD) studies

Absorption and MCD spectra associated with f–f transitions were measured in dichloromethane at room temperature. As seen in the previous study on the mononuclear phen and bpy complexes [17], the structural deformation found in the crystal structure would be defused in solution due to the flexible coordination bonds around Ln^{III} center. For instance, two dichloromethane solutions dissolving crystals of **2b**•$4CH_2Cl_2$ and **2b**•CH_2Cl_2 showed the identical spectra. Thus, we will discuss the spectroscopic properties of the bpm-bridged dithiocarbamato complexes with the ideal C_{2v} local symmetry at each Ln^{III} center. In Figures 5 and 6, the absorption and MCD spectra of Nd^{III}_2 and Eu^{III}_2 dithiocarbamato series of complexes are presented, respectively.

As shown in Figure 5*a* (top), the absorption spectrum of [{Nd(Me_2dtc)$_3$}$_2$(μ-bpm)] (**1a**) gives four sharp but weak f–f bands with their maximum at 12340, 13240, (16790, 16890) and 18762 cm^{-1}, assignable to the transition from the ground state $^4I_{9/2}$ to the excited states $^4F_{5/2}$, $^4S_{3/2}$, ($^4G_{5/2}$, $^2G_{7/2}$) and $^4G_{7/2}$, respectively. The intense band arising from the $^4I_{9/2}$ → ($^4G_{5/2}$, $^2G_{7/2}$) hypersensitive transition showed a weak splitting to 16790 and 16890 cm^{-1} with a pronged peak at 17090 cm^{-1}. In Figure 5*a* (bottom), the MCD signals at 12300, 13210, (16770,

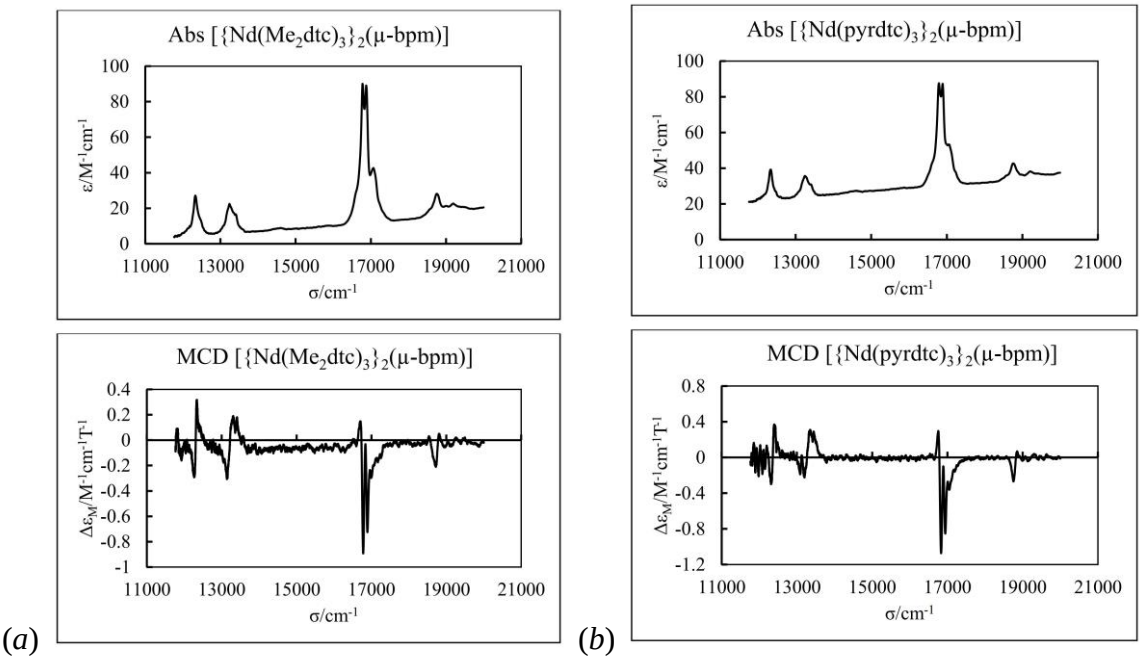

(*a*) (*b*)

Figure 5. Absorption (top) and MCD (bottom) spectra of (*a*) [{Nd(Me_2dtc)$_3$}$_2$(μ-bpm)] and (*b*) [{Nd(pyrdtc)$_3$}$_2$(μ-bpm)] complexes.

16890) and 18710 cm^{-1} correspond to the above-mentioned absorption bands. The MCD signals are dominated by room temperature *C*-terms except for that at 12340 cm^{-1} which appeared as a positive *A*-term. The characteristic $^4I_{9/2} \rightarrow (^4G_{5/2}, ^2G_{7/2})$ hypersensitive transition splits into a closely spaced *C*-terms at 16780 and 16890 cm^{-1}. Similar spectral features were observed for the [{Nd(pyrdtc)$_3$}$_2$(μ-bpm)] (**1b**) complex (Figure 5*b*).

In Figure 6*a* (top) the absorption spectrum of [{Eu(Me$_2$dtc)$_3$}$_2$(μ-bpm)] (**2a**) was shown, which exhibited a characteristic weak f–f bands at 21450 cm^{-1} assignable to the transition from the ground state $^7F_0$ to the excited state $^5D_2$. In the corresponding MCD spectrum (bottom), a characteristic negative *B*-term MCD signal is observed at 21450 cm^{-1}. Similar spectral features were observed for [{Eu(pyrdtc)$_3$}$_2$(μ-bpm)] (**2b**) (Figure 6*b*).

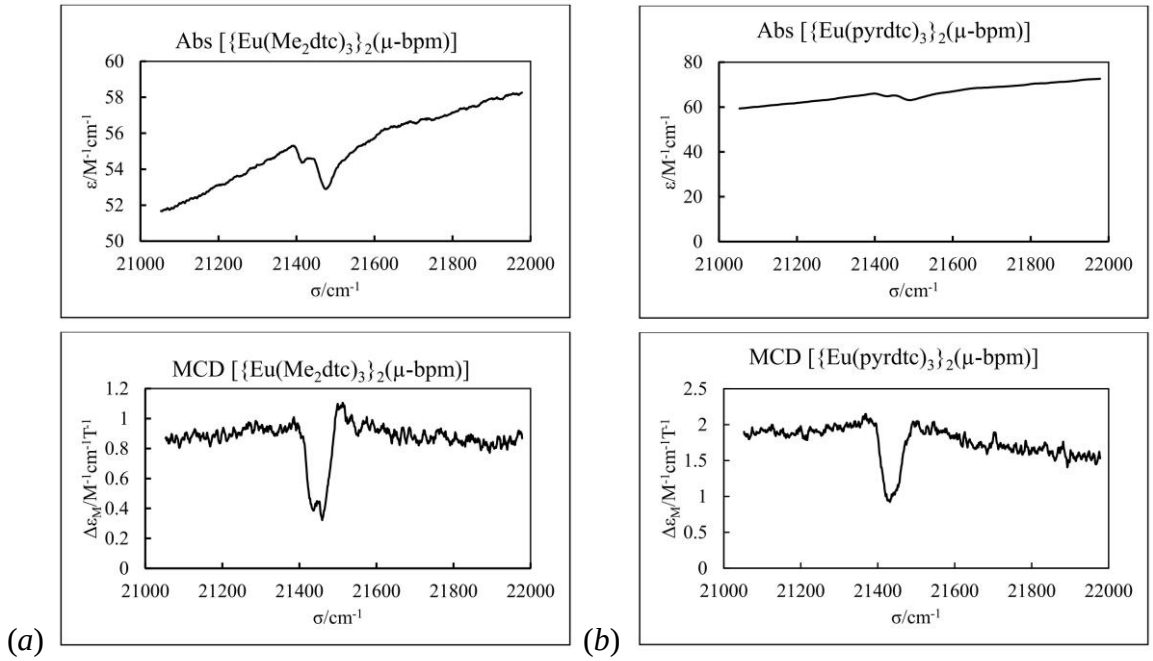

(*a*) (*b*)

Figure 6. Absorption (top) and MCD (bottom) spectra of (*a*) [{Eu(Me$_2$dtc)$_3$}$_2$(μ-bpm)] and (*b*) [{Eu(pyrdtc)$_3$}$_2$(μ-bpm)] complexes.

3.3.3 Spectral comparisons

Comparison of the absorption and MCD spectra of the bpm-bridged dinuclear complexes (Figures 5 and 6) to those of the mononuclear phen or bpy analogues [17] revealed very similar spectral features. This suggests that there is no significant $Ln^{III}\cdots Ln^{III}$ interaction in the

dinuclear complexes, which may induce a different electronic structure or spectroscopic symmetry around the central Ln^{III} ion.

For another spectral comparison, the *β*-diketonato analogues of [{Ln(acac)$_3$}$_2$(μ-bpm)] (Ln = Nd^{III} **1c** or Eu^{III} **2c**, $acac^-$ = 2,4-pentanedionate) were prepared and their absorption and MCD spectra were measured. The absorption and MCD spectra of **1c** are presented in Figure

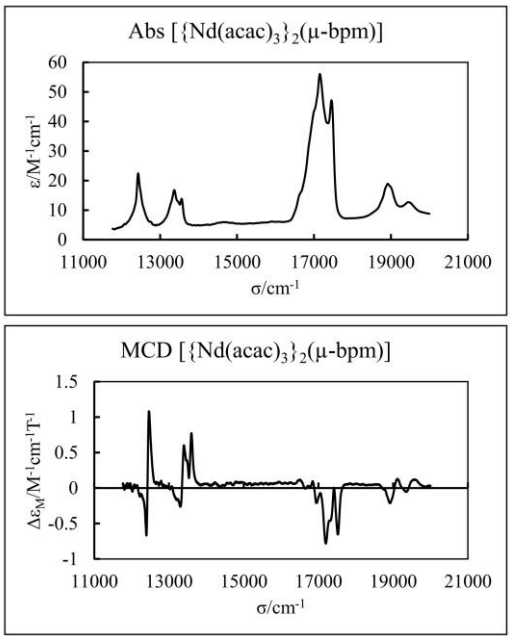

Figure 7. Absorption (top) and MCD (bottom) spectra of [Nd_2(acac)$_6$(μ-bpm)] (**1c**).

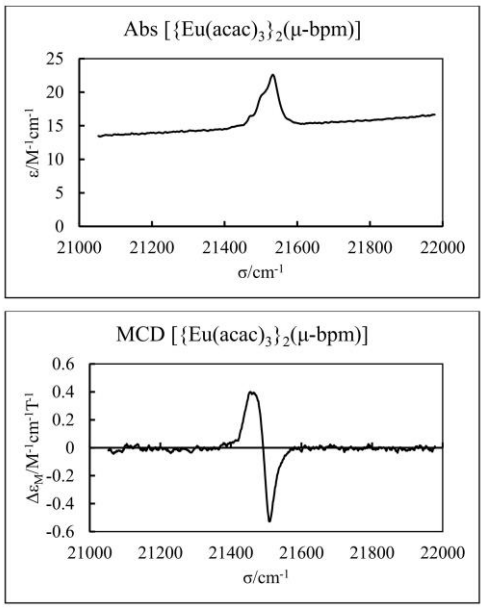

Figure 8. Absorption (top) and MCD (bottom) spectra of [{Eu(acac)$_3$}$_2$(μ-bpm)] (**2c**).

7, where a shape absorption band associated with the hypersensitive transition $^4I_{9/2} \rightarrow (^4G_{5/2}, ^2G_{7/2})$ at 17210 cm^{-1} is distinctively different from that of the dithiocarbamato complexes **1a** and **1b** (Figure 5). The room temperature *C*-terms in the MCD spectrum associated with the $^4I_{9/2} \rightarrow (^4G_{5/2}, ^2G_{7/2})$ transition at (17150, 17450 cm^{-1}) is more clearly resolved in **1c** than in complexes **1a** and **1b** (Figure 5). The Eu^{III} complex, $[\{Eu(acac)_3\}_2(\mu\text{-bpm})]$ (**2c**), on the other hand, exhibited a relatively intense absorption band and a negative *A*-term MCD signal at 21490 cm^{-1} assigned to the $^7F_0 \rightarrow {}^5D_2$ transition (Figure 8). This feature is a remarkable contrast to the dithiocarbamato complexes of **2a** and **2b**, which exhibited a very weak absorption band and a negative *B*-term MCD signals at 21450 cm^{-1} (Figure 6). A similar difference in the spectral features were observed in the previously reported mononuclear complexes [17], where we concluded that the electronic structure of Ln^{III} complexes may be largely related to the coordination environment of the central Ln^{III} ion. That is, also in the bpm-bridged dinuclear complexes, it is deduced that the dithiocarbamato and acetylacetonato complexes possess a C_{2v} and D_{2d} local symmetry, respectively [17].

4. Conclusion

In this study four new 2,2'-bipyrimidine (bpm)-bridged homodinuclear Ln^{III}_2 complexes bearing dithiocarbamato co-ligands have been prepared and their crystal structures have been analyzed. In the dinuclear complexes each Ln^{III} ion is 8-coordinated and situated in a distorted square antiprismatic geometry. Unlike to the corresponding mononuclear complexes with phen or bpy co-ligand, a severe distortion of one of the pyrdtc coordination structures was observed in some pseudo-polymorphs. The MCD spectral properties of the complexes were also investigated and found a distinctly different feature of the dithiocarbamato complexes from their β-diketonato analogues, owing to the coordination environment on the electronic structure and spectroscopic symmetry around the central Ln^{III} ions in solution.

Competing Interest

The authors declare no conflict of interest in relation to this work.

Appendix A. Supplementary data

Details of the crystal structures and the infrared spectra of the complexes in PDF format. CCDC nos. 1937579–1937584 contain the supplementary crystallographic data for compounds **1a**·2$CHCl_3$, **1b**·2$CHCl_3$, **2a**·2$CHCl_3$, **2b**·4CH_2Cl_2, **2b**·CH_2Cl_2 and **1c**. These data can be obtained free of charge via http://www.ccdc.cam.ac.uk/conts/retrieving.html or from The Cambridge Crystallographic Data Centre, 12 Union Read, Cambridge CB2 1EZ, UK; fax: (+44) 1223-336-033; or e-mail: deposit@ccdc.cam.ac.uk.

Acknowledgement

The authors wish to thank Dr. Yukinari Sunatsuki, for his assistance in the crystallographic analysis of the complexes. This work was supported by a Grant-in-Aid for Scientific Research No. 18K05146 from the Ministry of Education, Culture, Sports, Science, and Technology, Japan.

Reference

1. G. Zucchi, O. Maury, P. Thuery, M. Ephritikhine, *Inorg. Chem.,* 47 (2008) 10398.
2. S. Swavey, R. Swavey, *Coord. Chem. Rev.,* 253 (2009) 2627.
3. A. Fratini, G. Richards, E. Larder, S. Swavey, *Inorg. Chem.,* 47 (2008) 1030.
4. G. Zucchi, *Internat. J. Inorg. Chem.*, (2011) 1.
5. N. M. Shavaleev, G. Accorsi, D. Virgili, Z. R. Bell, T. Lazarides, G. Calogero, N. Armaroli, M. D. Ward, *Inorg. Chem.,* 44 (2005) 61.
6. M. D. Ward, T. Lazarides, H. Adams, D. Sykes, S. Faulkner, G. Calogero, *Dalton Trans.,* (2008) 691.
7. D. D'Cunha, D. Collins, G. Richards, S. Gilford G. S. Vincent, S. Swavey, *Inorg. Chem. Comm.,* 9 (2006) 979.
8. W. Yu, F. Schramm, E. M. Pineda, Y. Lan, O. Fuhr, J. Chen, H. Isshiki, W. Wernsdorfer, W. Wulfhekel, M. Ruben,. *Beilstein J. Nanotechnol.,* 7 (2016) 126.
9. W. -B. Sun, B. Yan, L. -H. Jia, B. -W. Wang, Q. Yang, X. Cheng, H. -F. Li, P. Chen, Z. -M. Wang, S. Gao, *Dalton Trans.,* 45 (2016) 8790.

10. R. Ilmi, K. Iftikhar, *Inorg. Chem. Comm.*, *13* (2010) 1552.
11. W.M. Faustino, O.L. Malta, E.E.S. Teotonio, H.F. Brito, A.M. Simas, G.F. de Sá, *J. Phys. Chem*., A110 (2006) 2510.
12. P. Pitchaimani, K.M. Lo, K.P. Elango, *Polyhedron*, 93 (2015) 8.
13. M.D. Regulacio, N. Tomson, S.L. Stoll, *Chem. Mater*., 17 (2005) 3114.
14. J. A. Vale, W. M. Faustino, P. H. Menezes, G. F. de Sá, *J. Braz. Chem. Soc.*, 17 (2006) 829.
15. P. Pitchaimani, K.M. Lo, K.P. Elango, *Polyhedron*, 54 (2013) 60.
16. V. Kubat, G. Demo, L. Jeremias, J. Novosad, *Z. Kristallogr.*, 228 (2013) 369.
17. A. Yakubu, T. Suzuki, M. Kita, *Inorg. Chim. Acta*, 484 (2019) 394.
18. Rigaku Co. Ltd., Process−Auto, Automatic Data Acquisition and Processing Package for Imaging Plate Diffractometer, Akishima, Tokyo, 1998.
19. C.M. Burla, R. Caliandro, M. Camalli, B. Carrozzini, L.G. Cascarano, L. De Caro, C. Giacovazzo, G. Polidori, D. Siliqi, R. Spagna, SIR2008. *J. Appl. Cryst.*, 40 (2007) 609.
20. M.G. Sheldrick, SHELXT Version 2014/5, *Acta Cryst.*, A70 (2014) C1437.
21. Rigaku Co. Ltd., CrystalStructure, Akishima, Tokyo, 2000−2014.
22. M.G. Sheldrick, SHELXL Version 2014/7, *Acta Cryst.*, A64 (2008) 112.
23. A. Yakubu, T. Suzuki, M. Kita. *J. Chem. Educ*., 94 (2017) 1357.
24. G. Zucchi, T. Jeon, D. Tondelier, D. Aldakov, P. Thuery, M. Ephritikhine, B. Geffroy, *J. Mater. Chem.*, 20 (2010) 2114.
25. A. Fratini, G. Richards, E. Larder, S. Swavey, *Inorg. Chem. Comm., 12* (2009) 509.
26. D. A. Brown, W. K. Glass, M. A. Burke. *Spectrochim. Acta*, 32A, (1976) 137.
27. I. Raya, I. Baba, B. M. Yamin. *Malaysia Journal of Analytical Sciences*, 10 (2006) 93.